SENSITIVITY OF PASSIVE MICROWAVE OBSERVATIONS TO SOIL MOISTURE FOR GROWING VEGETATION

K. C. Tien, J. Judge

ABSTRACT. *Root-zone soil moisture is one of the most crucial components driving surface hydrological processes. Crop growth models simulate these hydrological processes, such as energy and moisture fluxes in the root zone, and estimate crop development, biomass, and yield. Prediction of these fluxes can be improved significantly by using remotely sensed observations, particularly at microwave wavelengths. Microwave observations are highly sensitive to the moisture and temperature distributions in soil, with the sensitivity decreasing during a growing season as the vegetation biomass increases. This research focuses on understanding the sensitivities of microwave brightness signatures to changes in the soil moisture and temperature with increasing vegetation biomass.*

*In this article, the effects of changing soil moisture and temperatures on observed brightness temperatures (T_B) are discussed during a growing season of cotton (*Gossypium hirsutum*). These observed sensitivities from an extensive field experiment are compared with those obtained using a microwave emission model. The T_B at horizontal (H-) and (V-) vertical polarizations observed from the field experiment converged 50 days after planting corresponding to a LAI of 1.4, plant water content of 0.75 kg/m^2, and cotton height of 80 cm. The average sensitivities of the T_B to soil moisture changes in the early season from field observations were 2.0 and 1.0 K per percent volumetric moisture content (K·vol.%$^{-1}$) at H- and V-pol, respectively. These sensitivities to soil moisture compared well with those obtained by the emission model, viz, 2.98 and 1.35 K·vol.%$^{-1}$ at H- and V-pol, respectively. The observed sensitivities at both polarizations diminished when LAI was approximately 4.0 and plant water content (PWC) was approximately 1.5 kg·m^{-2}. The modeled sensitivities decreased significantly when PWC was greater than 0.8 kg·m^{-2}.*

Keywords. *Passive microwave remote sensing, Radiometer, Soil moisture, Vegetation properties, Cotton.*

Soil moisture in the root zone is one of the most important parameters for water and energy balance at the land surface and for crop growth. For example, the crop water stress is related to the crop evapotranspiration (ET), a function of the soil moisture (Oglesby, 1991; Cahill et al., 1999). Crop models such as CERES (Jones and Kiniry, 1986), CROPGRO (Boote et al., 1989), WOFOST (Supit et al., 1994), SWAP (van Dam et al., 1997), and STICS (Brisson et al., 2003) are used to simulate land surface fluxes and estimate crop development, biomass, and yield. Although the biophysics implemented in the models are well understood, the model flux estimates still diverge over time due to the accumulated errors in numerical approximations and model initialization (Reichle et al., 2002). One promising way to reduce the errors in flux estimates is to incorporate independent observations periodically into the model through data assimilation (McLaughlin, 2002; Crow and Wood, 2003; Heathman et al., 2003; Montaldo and Albertson, 2003; Aubert et al., 2003; Walker and Houser, 2004).

Submitted for review in June 2005 as manuscript number SW 5937; approved for publication by the Soil & Water Division of ASABE in November 2006.

The authors are **Kai-Jen Calvin Tien,** Graduate Student Research Assistant, and **Jasmeet Judge, ASABE Member Engineer,** Assistant Professor, Director, Center for Remote Sensing, Agricultural and Biological Engineering Department, University of Florida, Gainesville, Florida. **Corresponding author:** Jasmeet Judge, Center for Remote Sensing, Agricultural and Biological Engineering Dept., University of Florida, 266 Roger Hall, Gainesville, FL 32611; phone: 352-392-1864; fax: 352-392-4092; e-mail:jasmeet@ufl.edu.

Most of the recent efforts in using remote sensing techniques to improve crop growth estimates have been focused on relating the soil, vegetation, and other land surface properties using optical and near infrared remote sensing techniques. Wanjura and Upchurch (2000) used thermal infrared imagery to develop temperature-based indices to detect crop water stress. Senay et al. (1998) used airborne imagery whose spectral bands were from ultraviolet to thermal infrared along with Geographic Information System (GIS) and Digital Elevation Models (DEM) for precision farming. Plant et al. (2000) used Normalized Difference Vegetation Index (NDVI) calculated from the visible and infrared imagery to investigate the relations between the reflectance and growth and yield for cotton. Slaughter et al. (2001) used near-infrared data to measure soil moisture in the laboratory. Narasimhan et al. (2003) used spaceborne National Oceanic and Atmospheric Administration Advance Very High Resolution Radiometer (NOAA-AVHRR) imagery to estimate potential evapotranspiration.

Microwave remote sensing offers complementary observations to visible and infrared sensing. Unlike visible/infrared, microwave remote sensing can be used independent of solar illumination and under cloudy and low precipitation conditions. Due to longer wavelengths, microwave penetrates into the soil and vegetation canopy (Ulaby et al., 1981). In the presence of vegetation canopy, the radiance observed by the microwave sensors is a combination of contributions from the vegetation and the underlying surface soil. Passive microwave observations at low frequencies (< 10 GHz) are very sensitive to soil moisture in the top few centimeters in most vegetated surfaces, with the sensitivity decreasing as

  ISSN 0883–8542

vegetation biomass increases (Jackson et al., 1982; Schmugge, 1983; Jackson and Schmugge, 1991; Jackson, 1993; Njoku and Entekhabi, 1996). The observations are polarization dependent because reflectivity, hence emissivity, of terrain in the microwave region is primarily governed by its dielectric properties which are polarization dependent (Ulaby et al., 1981). For example, the microwave brightness at horizontal polarization (H-pol) is more sensitive to soil moisture changes than at vertical polarization (V-pol) (Njoku and O'Neill, 1982).

Over the past three decades, extensive theoretical and experimental research has been conducted using passive microwave observations to understand the interactions of the microwave signatures to the soil and vegetation properties. Hallikainen et al. (1985) and Dobson et al. (1985) used the field observations at 1.4 to 18 GHz (λ = 1.6 to 21 cm) to develop an empirical model for dielectric properties of the soil and water mixture. El-Rayes and Ulaby (1987) developed an empirical model for the dielectric properties of the vegetation canopy at 0.2 to 20 GHz (λ = 1.5 to 150 cm). Schmugge and Jackson (1992) developed an empirical microwave emission model for the vegetation canopy. Wigneron et al. (1996) used microwave observations at 1.4 (λ = 21 cm) and 5 GHz (λ = 6 cm) to monitor hydrological variables over agricultural land. Njoku and Li (1999) used passive microwave observations at 6 to 18 GHz (λ = 1.6 to 5 cm) to retrieve land surface parameters e.g. soil moisture, vegetation water content, and surface temperature. Judge et al. (1999) compared the brightness temperatures at 19 GHz (λ = 1.6 cm) observed by the microwave radiometer and the estimation by an integrated land surface process and microwave emission models. Jackson (2001) studied the relation between brightness temperatures at low frequency at 1.4 GHz (λ = 21 cm) and soil moisture over the spatial resolutions of 800 and 1600 m for the retrieval algorithms for the near-surface soil moisture. Calvet et al. (1996), Kerr et al. (2001), Njoku et al. (2003), and Drusch et al. (2004) used air- and space-borne passive microwave imagery at 1.4, 5.5, 6.9, and 36.5 GHz (λ = 21, 5.5, 4.4, and 0.8 cm) to retrieve soil moisture at regional scales. These studies demonstrate the need to understand interactions between the microwave brightness signatures and soil moisture in presence of dynamic vegetation.

The focus of this study is to investigate the sensitivities of microwave brightness temperatures (T_B) to changes in soil moisture and temperature for a growing season of cotton (*Gossypium hirsutum*). Observations from the first Microwave Water and Energy Balance Experiment (MicroWEX-1) were used to discuss changes in these sensitivities with growing vegetation. High temporal frequency of the season-long observations during MicroWEX-1 allowed for relating the effects of diurnal variations and sudden changes (due to rainfall or irrigation) in soil and terrain conditions on observed T_B. Because T_B are complex functions of moisture and temperature distributions, a simple microwave emission model is used to provide insight into sensitivities due to changes only in moisture or temperature. The modeled and observed sensitivities are discussed and compared during the season.

First Microwave Water and Energy Balance Experiment (MicroWEX-1)

MicroWEX-1 was conducted to collect a comprehensive dataset to gain a better understanding of the interactions among microwave brightness, soil moisture, and vegetation properties during a growing season of cotton. MicroWEX-1 was conducted by the Center for Remote Sensing, Department of Agricultural and Biological Engineering, University of Florida at the Plant Science Research and Education Unit [(PSREU), IFAS, Citra, Florida] (Tien et al., 2005). The cotton of variety Delta and Pineland Company Bollgard/Roundup Ready (DP555 BG/RR) was planted on 9 July 2003 (day of year, DOY 190) and harvested on 7 January 2004 (DOY 7). Figure 1a shows the locations of the 10,000-m^2 field site during MicroWEX-1 and figure 1b shows the layout of the sensors during MicroWEX-1. Brightness temperatures at 6.7 GHz (λ = 4.5 cm) were monitored by the tower-based University of Florida C-band Microwave Radiometer (UFCMR) every 30 min continuously from DOY 202 to 343 (see fig. 2a). Figures 2b and c show the front view of the antenna and side view of the rotary system. The UFCMR is a dual-polarized total power radiometer developed by the Microwave Geophysics Group at the University of Michigan. It observed the microwave brightness of an 11- × 11-m area on the ground from a height of 7.6 m.

A micrometeorological subsystem recorded soil moisture and temperature at depths of 4, 8, 12, and 20 cm using Vitel Hydra-probes, ground heat fluxes at depths of 4 and 8 cm, up- and down-welling solar and longwave radiation, thermal infrared temperature, and precipitation/irrigation every 15 min. An eddy covariance system was installed on DOY 227 to record the latent and sensible heat fluxes every 30 min. Table 1 shows the detailed information and location of the sensors. Weekly measurements of soil temperature and vegetation properties were conducted, including LAI. The LAI was measured by a plant canopy analyzer. The biomass of each component was obtained by weighing the leaves, stems, and bolls separately. The samples were dried in the oven at 75°C for 48 hours and weighed again. Figure 3 shows the V- and H-pol brightness signatures observed by the UFCMR during MicroWEX-1.

Microwave Emission Model

A microwave emission model simulates microwave brightness temperatures for given moisture and temperature distributions of a terrain. A simple terrain can be simulated as a semi-infinite soil with a vegetation layer above. The brightness temperature at polarization $p(T_{B,p})$ observed by a microwave radiometer for such a terrain includes three major components (as shown in fig. 4).

$$T_{B,p} = T_{B,atm,p} + T_{B,soil,p} + T_{B,canopy,p} \quad (1)$$

where $T_{B,atm,p}$, $T_{B,soil,p}$, and $T_{B,canopy,p}$ are the brightness temperature contributions from atmosphere, soil, and vegetation, respectively; $T_{B,p}$ is a function of moisture and temperature distributions in both the soil and the vegetation canopy.

Theory of radiative transfer can be used to estimate $T_{B,terrain,p}$ (Ulaby et al., 1981). Our model accounts for

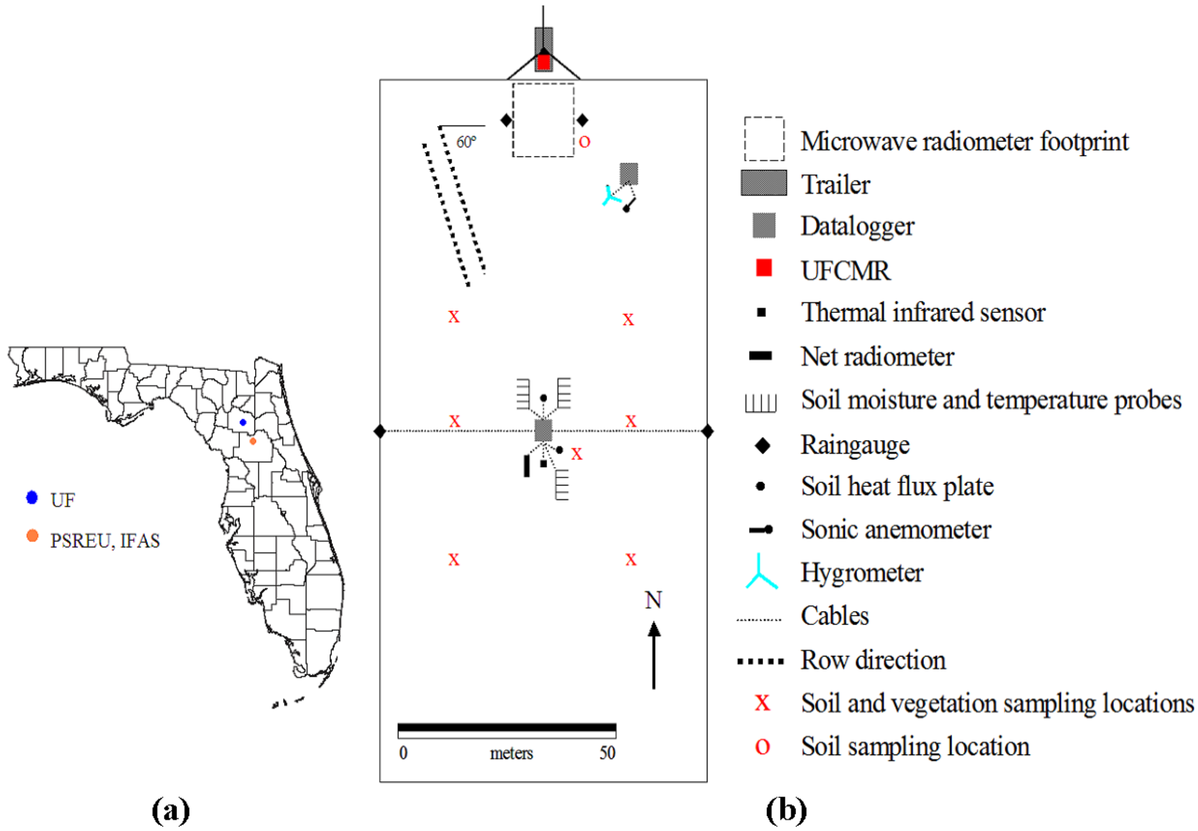

Figure 1. (a) Location of the MicroWEX-1 study site in the north central Florida and (b) layout of the sensors during MicroWEX-1.

non-scattering emission from atmosphere, vegetation, and soil layers as:

$$T_{B,terrain,p} = T_{B,sky}\Gamma_p \exp(-2\tau) + T_{soil}\left(1-\Gamma_p\right)\exp(-\tau) + T_{canopy}\left(1-\exp(-\tau)\right)\left(1+\Gamma_p \times \exp(-\tau)\right) \quad (2)$$

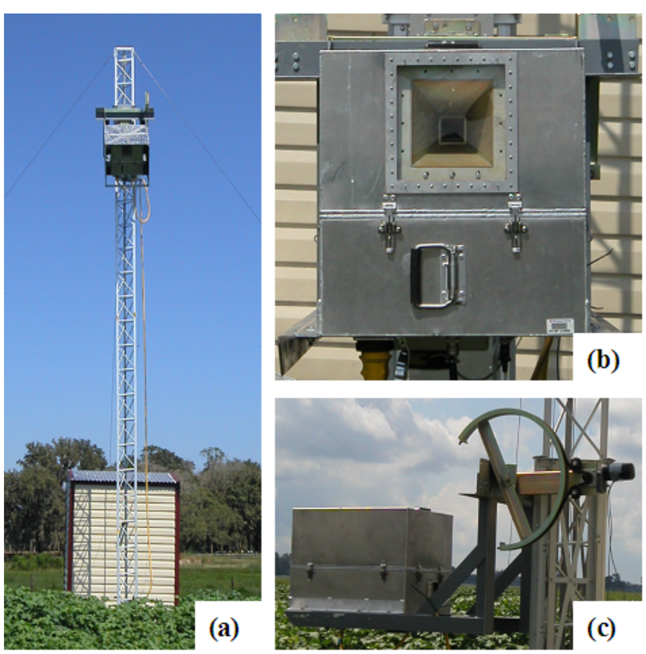

Figure 2. (a) University of Florida C-band Microwave Radiometer (UFCMR) field setup, (b) front view showing the antenna, and (c) side view showing the rotary system.

where $T_{B,sky}$ is the brightness temperatures of the sky; Γ_p is the reflectivity of the soil at polarization p; τ is the optical depth of the vegetation; T_{soil} is the effective physical temperature of the soil; T_{canopy} is the effective physical temperature of the vegetation. At 6.7 GHz (l = 4.5 cm), $T_{B,sky}$ is about 5 K (Ulaby et al., 1981).

Soil Emission Model

The soil is modeled as a semi-infinite, homogeneous, smooth-surfaced dielectric layer whose reflectivity at vertical (Γ_v) and horizontal (Γ_h) polarizations are given by Fresnel equations (Ulaby et al., 1981):

$$\Gamma_v(\theta) = \left|\frac{\varepsilon_{soil}\cos\theta - \sqrt{\varepsilon_{soil} - \sin^2\theta}}{\varepsilon_{soil}\cos\theta + \sqrt{\varepsilon_{soil} - \sin^2\theta}}\right|^2 \quad (3)$$

$$\Gamma_h(\theta) = \left|\frac{\cos\theta - \sqrt{\varepsilon_{soil} - \sin^2\theta}}{\cos\theta + \sqrt{\varepsilon_{soil} - \sin^2\theta}}\right|^2 \quad (4)$$

where θ is the incidence angle from zenith (see fig. 3), and ε_{soil} is the dielectric constant of the wet soil estimated by a dielectric mixing model (Dobson et al., 1985) as:

Table 1. Sensor descriptions during the MicroWEX-1.

Instrument	Vendor	Function	Position (m)
UFCMR	Microwave Geophysics Group, U. of Michigan	Brightness temperatures at 6.7 GHz	+ 7.6
CNR-1	Kipp & Zonen	Down- and up-welling short- and long-wave radiation	+ 2.5
Hydra probes	Stevens Water Monitoring System Inc.	Soil moisture and temperature	-0.04, -0.08, -0.12, -0.20
TDR probes	Campbell Scientific Inc.	Soil moisture	-0.04, -0.08, -0.12, -0.20
HFT-3	Campbell Scientific Inc.	Soil heat flux	-0.04, -0.08
CSAT3 and KH20	Campbell Scientific Inc.	Latent and sensible heat fluxes and wind direction	+ 2.1
4000.3ZL	Everest Interscience Inc.	Thermal infrared temperature	+ 2.5
Raingauges	Forestry Supplier Inc.	Rainfall	+ 2.0
LAI-2000	Li-Cor Biosciences	Leaf Area Index	---

$$\varepsilon_{soil}^{\alpha} = v_{ss}\,\varepsilon_{ss}^{\alpha} + v_a\,\varepsilon_a^{\alpha} + v_{fw}\,\varepsilon_{fw}^{\alpha} + v_{bw}\,\varepsilon_{bw}^{\alpha} \qquad (5)$$

where v and ε are the volumetric fractions [$m^3 \cdot m^{-3}$] and dielectric constants, respectively. The subscripts *ss*, *a*, *fw*, and *bw* refer to soil solids, air, free water, and bound water, respectively; α is the scale factor equal to 0.65 in the model; v_{fw} is estimated as the volumetric soil moisture (VSM); ε_{fw} is estimated using Debye equation at soil temperature of 300 K (Ulaby et al., 1986); v_{bw} is assumed to be zero because its value is very small for sandy soils (Dobson et al., 1985). The values for ε_{ss}, ε_a, ε_{fw}, and v_{ss} used in the model were 4.75-j0.23, 1.0, 70.6-j22.4, and 0.55, respectively, where j = $\sqrt{-1}$. The effective temperature of soil was assumed to be isothermal at 300 K, similar to the observed average temperature.

Vegetation Emission Model

Vegetation serves as an absorbing/emitting layer above the soil. A non-scattering canopy can be modeled as a homogeneous dielectric layer (cloud) with only absorption and emission occurring within the canopy. The absorption in the canopy is determined by its optical depth τ, which is a function of the dielectric and biophysical properties of the canopy (Ulaby et al., 1981).

$$\tau = -2k_0 \int_0^{hc} \mathrm{Im}\left[n_t\right] dz \qquad (6)$$

where k_0 is the vacuum wave number [m^{-1}]; h_c is the height of canopy; n_t is the total index of refraction of air-vegetation mixture as (England and Galantowicz, 1995):

$$n_t = 1 + v_c \sqrt{\varepsilon_c} \qquad (7)$$

where v_c and ε_c are the volume fraction and dielectric constant of the wet canopy, respectively. The dielectric constant of the wet canopy is estimated as (Ulaby and El-Rayes, 1987):

$$\varepsilon_c = \varepsilon_r + v_{fw}\,\varepsilon_{fw} + v_{bw}\,\varepsilon_{bw} \qquad (8)$$

where v and ε are the volumetric moisture content [$m^3 \cdot m^{-3}$] and dielectric constant, respectively. The subscript *r* refers to residual water. ε_{fw} and ε_{bw} are functions of frequency, *f* [GHz] as (Ulaby and El-Rayes, 1987):

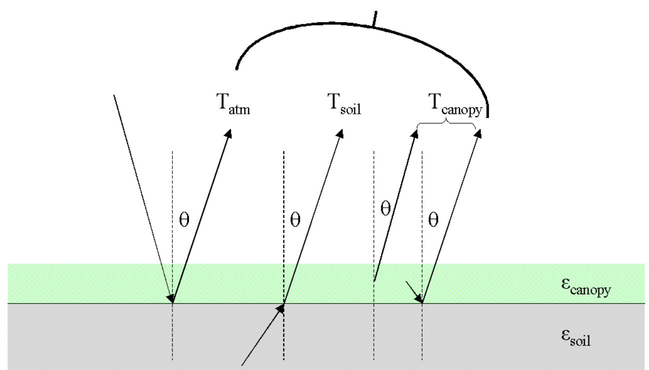

Figure 4. Zero order radiative transfer model for soil and canopy.

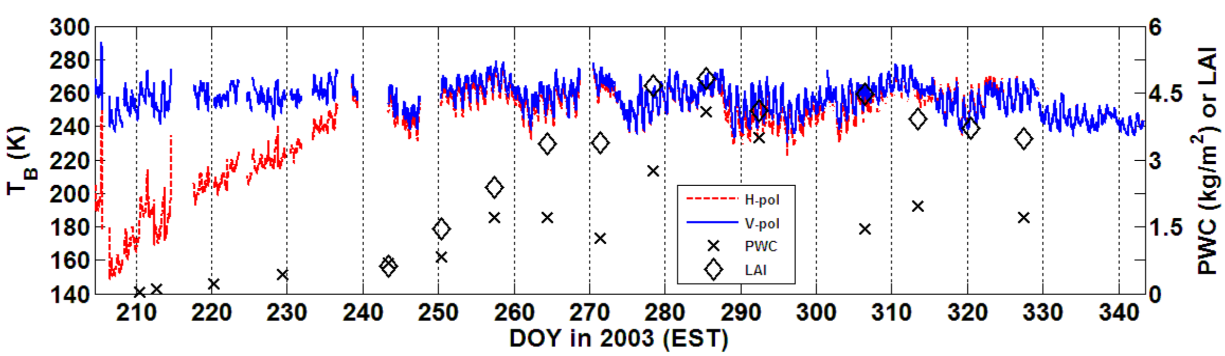

Figure 3. Microwave brightness temperatures at V- and H-pol with LAI and plant water content.

$$\varepsilon_{fw} = 4.9 + \frac{75}{1 + j\frac{f}{18}} - j\,\frac{22.86}{f} \quad (9)$$

$$\varepsilon_{bw} = 2.9 + \frac{55}{1 + \sqrt{j\,\frac{f}{0.18}}} \quad (10)$$

At room temperature, ε_r, ν_{fw}, and ν_{bw} for the canopy are given in terms of plant water content (PWC) as (Ulaby et al., 1986):

$$\varepsilon_r = 1.7 + 3.2\frac{\sigma_{veg}}{\rho_c} + 6.5\left(\frac{\sigma_{veg}}{\rho_c}\right)^2 \quad (11a)$$

$$v_{fw} = \frac{\sigma_{veg}}{\rho_c}\left(0.82\frac{\sigma_{veg}}{\rho_c} + 0.166\right) \quad (11b)$$

$$v_{bw} = \frac{3.14\left(\frac{\sigma_{veg}}{\rho_c}\right)^2}{1 + 59.5\left(\frac{\sigma_{veg}}{\rho_c}\right)^2} \quad (11c)$$

where σ_{veg} is PWC [kg·m^{-2}] and ρ_c is the density of the dry vegetated material per unit area [kg·m^{-2}]. In the model, ρ_c was equal to the observed value of 0.6 kg·m^{-2}. The canopy was assumed isothermal at 300 K, similar to the observed average temperature during the growing season of cotton.

The model was used to calculate H- and V-pol T_B with incremental increases in VSM during the growing season as PWC increased from 0 (bare soil) to 1.0 kg·m^{-2} (mature cotton). The incremental increases in VSM ranged from very dry soil to saturated soil, at 10%, 20%, 30%, and 40%. Figures 5a and b show the sensitivities of the T_B at H- and V-pol to changes in soil moisture over the growing season as estimated by the microwave emission model. H-pol is more sensitive to soil moisture than V-pol. The T_B are the most sensitive to soil moisture changes in bare soil conditions and when the soil is dry. The sensitivity decreases linearly with increasing soil wetness for H-pol, whereas the decrease is not linear for V-pol (see figs. 5a and b). The sensitivity of the T_B at H-pol was 7.8 K·vol.%$^{-1}$ for dry soil and the sensitivity decreased to 1.3 K·vol.%$^{-1}$ for saturated soil (see fig. 5 a). The sensitivity of the T_B at V-pol was low at 1.3 K·vol.%$^{-1}$ for very dry soil, increased to its maximum of 2.0 K·vol.%$^{-1}$ at VSM = 20%, and decreased to 1.6 K·vol.%$^{-1}$ (see fig. 5b). The sensitivity was maximum at 20 % VSM because the reflectivity at V-pol is a second order function of dielectric property of the soils (see eq. 3), with the smallest value of ε_{soil} occurring at VSM = 20%. The sensitivity of the T_B to soil moisture decreased significantly for both polarizations when vegetation water content was > 1.0 kg·m^{-2} for dry condition and 0.8 kg·m^{-2} for wet condition.

Figure 5c shows the sensitivity of modeled T_B to changes in effective physical temperature of bare soil (T_{eff}) when PWC = 0 as the volumetric moisture content increases from 0 to 40%. The T_B is simulated using the microwave emission model described earlier. The sensitivity of T_B to changes in effective temperature is obtained by calculating the differences between the T_B at the effective temperatures of 300 and 301 K from 0 to 40% VSM. The sensitivity of T_B to T_{eff} is approximately 1 K·K^{-1} at V-pol and 0.8 K·K^{-1} at H-pol under dry soil condition, while the sensitivity of T_B to T_{eff} decreases to 0.76 K·K^{-1} at V-pol and 0.38 K·K^{-1} at H-pol under wet soil condition.

Results and Discussion

The MicroWEX-1 was a unique experiment to measure T_B at 6.7 GHz concurrently with observations of water and energy fluxes. The T_B at H-pol were lower than that at V-pol early in the season and rapidly increased with the increasing contribution from the growing vegetation (fig. 3). The lowest T_B at H-pol was around 160 K on DOY 206.5 at the beginning of the season. The H-pol T_B reached 260 K on DOY 240. Before DOY 240, the land surface was sparsely vegetated and the canopy contribution was minimal. The difference in T_B at H- and V-pol before DOY 240 was primarily due to low emissivities at H-pol rather than those at V-pol. The maximum difference between the T_B at two polarizations was 90 K.

The T_B at V- and H-pol converged on DOY 240, 50 days after planting corresponding to LAI of 1.4, PWC of 0.75 kg·m^{-2} (see fig. 3), and the canopy height of 80 cm. After DOY 240, a maximum difference of 10 K between the T_B at two polarizations was observed. The overall T_B values at both polarizations were dominated by emission from the canopy. Most of the polarization dependent energy emitted from the soil was attenuated by the vegetation canopy, and the observed T_B were primarily due to emission from the canopy. The canopy emission was polarization independent because the moisture distribution within the canopy was statistically random at 6.7 GHz, resulting in similar T_B at the two polarizations.

The T_B values at H-pol were more sensitive to changes in moisture than at V-pol for bare soil (Njoku and O'Neill, 1982). This is because V-pol primarily responds to soil temperature fluctuations at the incidence angle of 55°, close to the Brewster angle at microwave frequencies. The sensitivities of the T_B at V- and H-pol to the surface soil moisture decreased during the experiment as the canopy contribution increased. The T_B at both polarizations responded to the precipitation and/or irrigation in the early growing season. For example, the T_B at H- and V-pol decreased by 70 and 40 K, respectively, on DOY 205.5, corresponding to an increase in the VSM of 25% at 4 cm depth (fig. 6). Because T_B is a function of both T_{eff} and VSM, a part of the observed decrease in T_B was due to a change in T_{eff}. During the increase in VSM, from 12 % to 36 %, soil temperatures decreased by 11 K. The changes in T_B due to changes in T_{eff} were estimated to be approximately 7 and 10 K at H- and V-pol from figure 5c. This would result in a $\Delta T_B \cdot \Delta VSM^{-1}$ of 2.5 and 1.2 K·vol.%$^{-1}$ for DOY 205.5. An intermediate response of about 20 K at H-pol and 15 K at V-pol on DOY 206.5 was observed for an increase of approximately 10% in volumetric soil moisture. Accounting for the 2.0 K decrease in T_{eff}, the $\Delta T_B \cdot \Delta VSM^{-1}$ for DOY 206.5 was 1.5 and 0.7 K·vol.%$^{-1}$ at H- and V-pol, respectively. Similar responses were also observed on DOY 212.5 and 213.8 corresponding to an increase of about 15%.

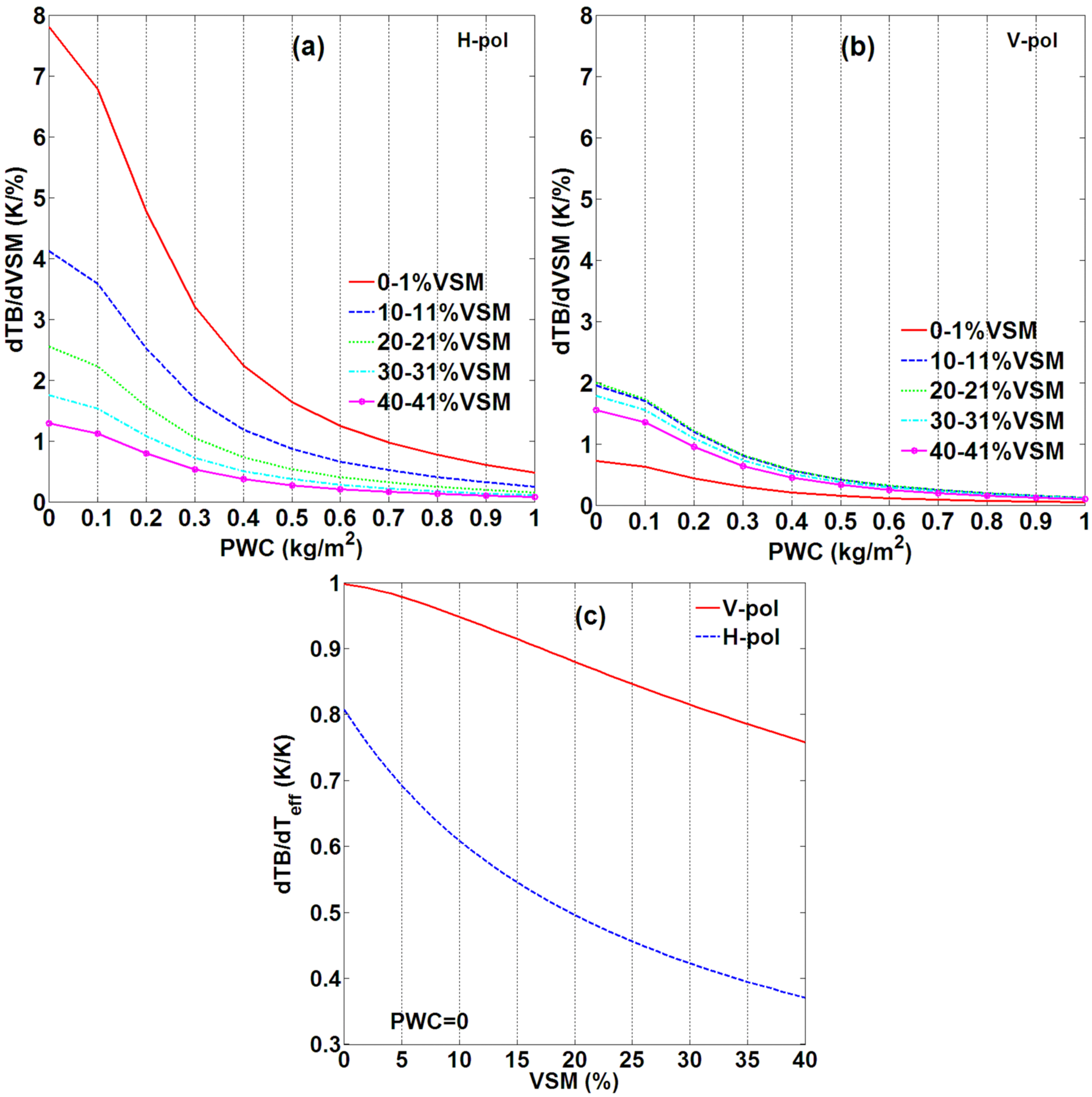

Figure 5. Sensitivity of the model brightness temperatures to changes in volumetric soil moisture at different PWC at (a) H-pol, (b) V-pol, and (c) sensitivity of brightness temperatures to effective physical temperature of soil when PWC = 0.

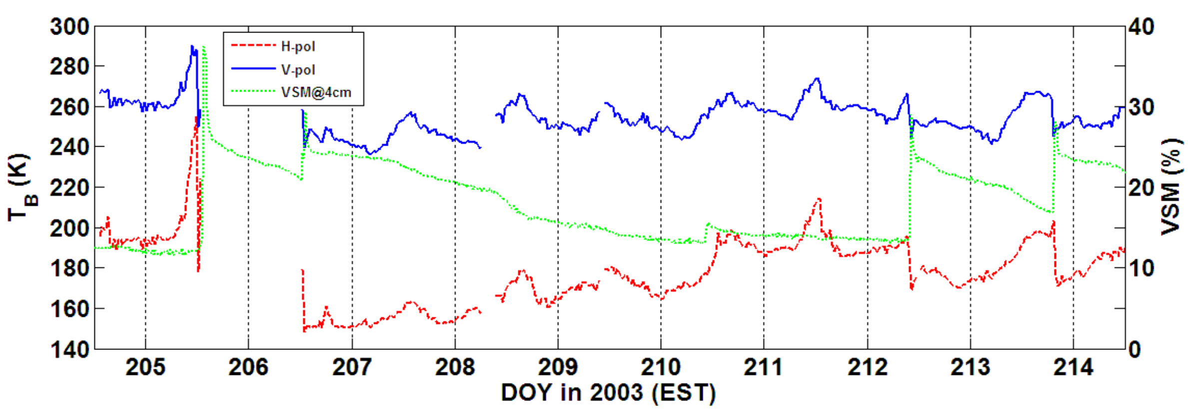

Figure 6. Response of brightness temperatures at V- and H-pol to the soil moisture changes at 4 cm during the early season.

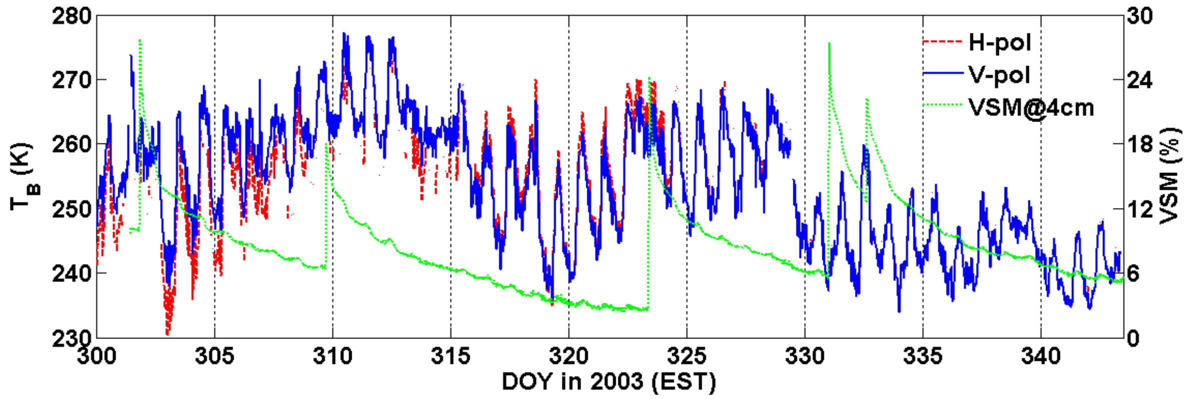

Figure 7. Response of brightness temperatures of V- and H-pol to the soil moisture changes at 4 cm during the late season.

In the late season, the T_B were dominated by emission from vegetation canopy and were less sensitive to changes in soil moisture. The T_B did not respond significantly to increases of 20%, 10%, and 20 % in VSM on DOY 302, 310, and 323, respectively (fig. 7). The sensitivities of the T_B to the changes in soil moisture from the MicroWEX-1 matched the sensitivities of 2.98 K·vol.%$^{-1}$ and 1.35 K·vol.%$^{-1}$ at H and V-pol as derived by the microwave brightness model in the early season. When the PWC was greater than 0.8 kg·m^{-2}, the sensitivities of the modeled T_B to the changes in soil moisture were less than 0.4 K·vol.%$^{-1}$ at H-pol and 0.2 K·vol.%$^{-1}$ at V-pol, similar to those observed during MicroWEX-1.

Conclusion

The field experiment MicroWEX-1 was designed to understand the interactions between microwave brightness, soil moisture, and vegetation properties for a growing season of cotton. In this study, observations from MicroWEX-1 are used to estimate the sensitivities of T_B to soil moisture and temperature over the growing season of cotton. The observed sensitivities of T_B at H-pol in the early season were at an average value of 2.0 K·vol.%$^{-1}$, while those at V-pol was at an average value of 1.0 K·vol.%$^{-1}$. The modeled sensitivities were similar to the observed values of 2.98 K·vol.%$^{-1}$ at H-pol and 1.35 K·vol.%$^{-1}$ at V-pol in the early season. The observed sensitivities of the T_B to the changes in soil moisture at 4 cm matched well with the modeled sensitivities in the early season. The microwave observations at C-band were not sensitive to changes in VSM at 4 cm in the late season when LAI was approximately 4.0 and PWC was 1.5 kg·m^{-2}. The modeled sensitivities decreased significantly when PWC was greater than 0.8 kg·m^{-2}.

Acknowledgements

Funding for this research was provided by the NASA Earth System Science Graduate Student Fellowship program (Award #: ESSF03-0000-0044) and internal funds from the Institute of Food and Agricultural Sciences, University of Florida. The authors would also like to thank Mr. Larry Miller and Orlando Lanni for their expert engineering support during MicroWEX-1; the PSREU Research Coordinator Mr. Jim Boyer and his team for providing excellent management of cotton; Dr. Jennifer Jacobs at the University of New Hampshire for providing the Eddy Covariance System during MicroWEX-1; Dr. Michael Dukes at the University of Florida for providing the air pressure, temperature, and relative humidity data used in the UFCMR calibration.

References

Aubert, D., C. Loumagne, and L. Oudin. 2003. Sequential assimilation of soil moisture and streamflow data in a conceptual rainfall-runoff model. *J. Hydrol.* 280(2): 145-161.

Boote, K. J., J. W. Jones, G. Hoogenboom, G. G. Wilkerson, and S. S. Jagtap. 1989. PNUTGRO v1.02. Peanut Crop Growth Simulation Model, Users Guide. Florida Agricultural Experiment Station Model No. 8420. University of Florida, Gainesville, Fla.

Brisson, N., C. Gary, E. Justes, R. Roche, B. Mary, D. Ripoche, D. Zimmer, J. Sierra, P. Bertuzzi, P. Burger, F. Bussiere, Y. M. Cabidoche, P. Cellier, P. Debaeke, J. P. Gaudillere, C. Henault, F. Maraux, B. Seguin, and H. Sinoquet. 2003. An overview of the crop model STICS. *Europ. J. Agronomy* 18(3): 309-332.

Cahill, A. T., M. B. Parlange, T. J. Jackson, P. E. O 'Neill, and T. J. Schmugge. 1999. Evaporation from nonvegetation surfaces: surface aridity methods and passive microwave remote sensing. *IEEE Trans. Geo. Remote Sensing* 38(9): 1346-1351.

Calvet, J. C., A. Chanzy, and J. P. Wigneron. 1996. Surface temperature and soil moisture retrieval in the Sahel from airborne multifrequency microwave radiometry. *IEEE Trans. Geo. Remote Sensing* 34(2): 588-600.

Crow, W. T., and E. F. Wood, 2003. The assimilation of remotely sensed soil brightness temperatures imagery into a land surface model using Ensemble Kalman filtering: A case study based on ESTAR measurements during SGP97. *Adv. Water Resources* 26(2): 137-149.

Dobson, M. C., F. T. Ulaby, M. T. Hallikainen, and M. A. El-Rayes. 1985. Microwave dielectric behavior of wet soil-part II: Dielectric mixing models. *IEEE Trans. Geo. Remote Sensing* 23(1): 35-46.

Drusch, M., E. F. Wood, H. Gao, and A. Thiele. 2004. Soil moisture retrieval during the Southern Great Plain Hydrology Experiment 1999: a comparison between experimental remote sensing data and operational products. *Water Resource Research* 40: W02504, doi:10.1029/2003WR002441.

El-Rayes, M. A., and F. T. Ulaby. 1987. Microwave dielectric spectrum of vegetation-part I: experimental observations. *IEEE Trans. Geo. Remote Sensing* 25(5): 541-549.

England, A. W. and J. F. Galantowicz. 1995. Observed and modeled radiobrightness of prairie grass in early fall. In *Proc. Internal Geoscience And Remote Sensing Symposium 1995*. New York: IEEE.

Hallikainen, M. T., F. T. Ulaby, M. C. Dobson, M. A. El-Rayes, and L. Wu. 1985. Microwave dielectric behavior of wet soil-part I: empirical models and experimental observations. *IEEE Trans. Geo. Remote Sensing* 23(1): 25-34.

Heathman, G. C., P. J. Starks, L. R. Ahuja, and T. J. Jackson. 2003. Assimilation of surface soil moisture to estimate profile soil water content. *J. Hydrol.* 279(1): 1-17.

Jackson, T. J., T. J. Schmugge, and J. R. Wang. 1982. Passive microwave sensing of soil-moisture under vegetation canopy. *Water Resour. Res*. 18(4): 1137-1142.

Jackson, T. J., and T. J. Schmugge. 1991. Vegetation effects on the microwave emission of soils. *Remote Sensing Enviorn.* 36(3): 203-212.

Jackson, T. J. 1993. Measuring surface soil moisture using passive microwave remote sensing. *Hydro. Proc.* 7(2): 139-152.

Jackson, T. J. 2001. Multiple resolutions of L-band brightness temperatures for soil moisture. *IEEE Trans. Geo. Remote Sensing* 39(1): 151-164.

Jones, C. A., and J. R. Kiniry. 1986. *CERES-Maize: A Simulation Model of Maize Growth and Development*. College Station, Tex.: Texas A&M Press.

Judge, J., A. W. England, W. L. Crosson, C. A. Laymon, B. K. Hornbuckle, D. L. Borie, E. J. Kim, and Y. Liou. 1999. A growing season land surface process/radiobrightness model for wheat-stubble in the Southern Great Plain. *IEEE Trans. Geo. Remote Sensing* 37(5): 2152-2158.

Kerr, Y. H., P. Waldteufel, J. P. Wigneron, J. M. Martinuzzi, J. Font, and M. Berger. 2001. Soil moisture retrieval from space: The Soil Moisture and Ocean Salinity (SMOS) mission. *IEEE Trans. Geo. Remote Sensing* 39(8): 1729-1735.

McLaughlin, D. 2002. An integrated approach to hydrologic data assimilation: Interpolation, smoothing, and filtering. *Adv. Water Resources* 25(3): 1275-1286.

Montaldo, N., and J. D. Albertson. 2003. Multi-scale assimilation of surface soil moisture data for robust root zone moisture predictions. *Adv. Water Resources* 26(1): 33-44.

Narasimhan, B., R. Srinivasan, and A. D. Whittaker. 2003. Estimation of potential evapotranspiration from NOAA-AVHRR satellite. *Applied Engineering in Agriculture* 19(3): 309-318.

Njoku, E. G., and P. E. O 'Neill. 1982. Multifrequency microwave radiometer measurements of soil-moisture. *IEEE Trans. Geosci. Remote Sensing* GE20(4): 468-475.

Njoku, E. G., and D. Entekhabi. 1996. Passive microwave remote sensing of soil moisture. *J. Hydrol.* 184(1): 101-129.

Njoku, E. G., and L. Li. 1999. Retrieval of land surface parameters using passive microwave measurements at 6-18 GHz. *IEEE Trans. Geo. Remote Sensing* 37(1): 79-93.

Njoku, E. G., T. J. Jackson, V. Lakshmi, T. K. Chan, and S. V. Nghiem. 2003. Soil moisture retrieval from AMSR-E. *IEEE Trans. Geo. Remote Sensing* 41(2): 215-229.

Oglesby, R. J. 1991 Springtime soil moisture, natural climate variability and North American drought as simulated by NCAR community model 1. *J. Climate* 4(9): 890-897.

Plant, R. E., D. S. Munk, B. R. Roberts, R. L. Vargas, D. W. Rains, R. L. Travis, and R. B. Hutmacher. 2000. Relationships between remotely sensed reflectance data and cotton growth and yield. *Transactions of the ASAE* 43(3): 535-546.

Reichle, R. H., J. P. Walker, R. D. Koster, and P. R. Houser, 2002. Extended versus Ensemble Kalman Filtering for land data assimilation. *J. Hydrometeorology* 3(6): 728-740.

Schmugge, T. J. 1983. Remote-sensing of soil-moisture with microwave radiometers. *Transactions of the ASAE* 26(3): 748-753.

Schmugge, T. J., and T. J. Jackson. 1992. A dielectric model of the vegetation effects on the microwave emission from soils. *IEEE Trans. Geo. Remote Sensing* 30(4): 757-760.

Senay, G. B., A. D. Ward, J. G. Lyon, N. R. Fausey, and S. E. Nokes. 1998. Manipulation of high spatial resolution aircraft remote sensing data for use in site-specific farming. *Transactions of the ASAE* 41(2): 489-495.

Slaughter, D. C., M. G. Pelletier, and S. K. Upadhyaya. 2001. Sensing soil moisture using NIR spectroscopy. *Applied Engineering in Agriculture* 17(2): 241-247.

Supit, I., A. A. Hooijer, and C. A. van Diepen. 1994. System description of the WOFOST 6.0 crop simulation model implemented in CGMS, vol. 1: Theory and algorithms. Joint Research Center, Commission of the European Communities, EUR 15956 EN, Luxembourg.

Tien, K. C., J. Judge, O. Lanni, and L. Miller. 2005. The first Microwave Water and Energy Balance Experiment (MicroWEX-1) Experimental field report. Citra, Fla.: Center for Remote Sensing, UF/IFAS. Available at http://edis.ifas.ufl.edu/AE288. Accessed 1 April 2006.

Ulaby, F. T., and M. A. El-Rayes. 1987. Microwave dielectric spectrum of vegetation-part II: Dual-dispersion model. *IEEE Trans. Geo. Remote Sensing* 25(5): 550-556.

Ulaby, F. Y., R. K. Moore, and A. K. Fung. 1981. *Microwave Remote Sensing: Active and Passive*, Vol. I, Norwood, Mass.: Artech House.

Ulaby, F. Y., R. K. Moore, and A. K. Fung. 1986. *Microwave Remote Sensing: Active and Passive*, Vol. III, Norwood, Mass.: Artech House.

van Dam, J. C., J. Huygen, J. G. Wesseling, R. A. Feddes, P. Kabats, P. E. V. van Walsum, P. Groenendijk, and C. A. van Diepen. 1997. Theory of SWAP version 2.0, Report #71. Department Water Resources, Wageningen Agricultural Univeristy.

Walker, J. P., and P. R. Houser. 2004. Requirements of a global near-surface soil moisture satellite mission: Accuracy, repeat time, and spatial resolution. *Adv. Water Resources* 27(8): 785-801.

Wanjura, D. F., and D. R. Upchurch. 2000. Canopy temperature characterizations of corn and cotton water status. *Transactions of the ASAE* 43(4): 867-875.

Wigneron, W. P., J. C. Calvet, and Y. Kerr. 1996. Monitoring water interception by crop fields from passive microwave observations. *Agric. Forest Meteol.* 80(2): 177-194